Superoxide and Nitrous Acid Production from Nitrate Photolysis Is Enhanced by Dissolved Aliphatic Organic Matter

Xinke Wang, Evan Dalton, Zachary Payne, Sébastien Perrier, M. Riva, Jonathan Raff, C. George

Superoxide and nitrous acid production from nitrate photolysis is enhanced by dissolved aliphatic organic matter

Xinke Wang,[†,#] Evan Z. Dalton,[‡,#] Zachary C. Payne,[‡] Sebastien Perrier,[†] Matthieu Riva,[†] Jonathan D. Raff,[‡,§,*] and Christian George[†,*]

[†]Univ Lyon, Université Claude Bernard Lyon 1, CNRS, IRCELYON, F-69626, Villeurbanne, France.

[‡]Department of Chemistry, Indiana University, 800 East Kirkwood Avenue, Bloomington, Indiana 47405, United States.

[§]O'Neill School of Public and Environmental Affairs, Indiana University, 1315 East 10th Street, Bloomington, Indiana 47405, United States

[*]To whom correspondence should be addressed. Email: christian.george@ircelyon.univ-lyon1.fr, jdraff@indiana.edu

[#]These authors contributed equally to this work

ABSTRACT: Nitrate anion (NO_3^-) is ubiquitous in the environment and its photochemistry produces nitrous acid (HONO), a major source of tropospheric hydroxyl radical (OH). Enhanced $HONO_{(g)}$ emissions have been observed from $NO_3^-{}_{(aq)}$ photolysis in field studies, although the underlying reasons for this enhancement are debated. Here, we show that the enhancement is induced by changes in secondary nitrate anion photochemistry due to dissolved aliphatic organic matter (DAOM). Increased yields of superoxide radical (O_2^-) and HONO were observed when NO_3^- solutions (pH 6) were photolyzed in the presence of DAOM surrogates of varying solubility. An additional experiment titrated with additional DAOM showed a further increase in $O_2^-{}_{(aq)}$ and $HONO_{(g)}$ simultaneously with decreased yields of gaseous nitric oxide (NO) and nitrogen dioxide (NO_2). To our knowledge, this is the first time that superoxide was directly observed as an intermediate in nitrate photolysis experiments, produced through DOAM oxidation by $OH_{(aq)}$. Herein, we suggest that enhanced HONO(g) emissions from NO_3^-(aq) photolysis result from the reaction of $O_2^-{}_{(aq)}$ with $NO_{2(aq)}$ and $NO_{(aq)}$ to respectively form peroxynitrate ($OONO_2^-$) and peroxynitrite ($OONO^-$), which are precursors to nitrite (NO_2^-). Overall, this points to an important role of O_2^- in aqueous aerosol chemistry, which is currently under-appreciated.

INTRODUCTION

Nitrate anion (NO_3^-) is a ubiquitous, photochemically-active compound in the atmospheric condensed phase, surface water, and on boundary layer surfaces. The photochemistry of nitrate anions has been extensively studied over the last decades due to its importance as a major source of aqueous hydroxyl radical (OH).[1,2] Several studies have shown that pH, nitrate concentration and the presence of organic OH scavengers play important roles in the nitrite yield, which lead to the large variations in the measured values of the quantum yield $\Phi(NO_2^-)$ from 0.2% to 4%.[3–6] Benedict

et al.[5] showed that $\Phi(NO_2^-)$ is constant at high pH, but decreases with decreasing pH in more acidic solutions (pH < 5) due to $HONO_{(aq)}$ loss to the gas phase[4] or less effective scavenging of $OH_{(aq)}$ by bicarbonate/carbonate. Therefore, nitrite and NO_2 quantum yields must be assessed in the presence of organic OH scavengers, which prevent conversion of aqueous NO_2^- and NO_2 back into NO_3^- by OH radicals.[4,7] While the influence of OH scavengers on the primary products of nitrate photolysis is well established, the impact of organic matter on secondary nitrate photoproducts is poorly understood.

Factors that affect $NO_2^-{}_{(aq)}$ yields influence daytime $HONO_{(g)}$ concentrations in the lower troposphere. Photolysis of $HONO_{(g)}$ is a major daytime source of $OH_{(g)}$ radicals that accelerates photochemical transformations leading to pollutant degradation and the formation of aerosols and tropospheric ozone.[8–10] Various $HONO_{(g)}$ sources have now been identified, including soil bacteria and fuel combustion,[11,12] gas phase reaction between OH and NO,[13,14] photosensitized conversion of NO_2 on surfaces,[15,16] and heterogeneous conversion of NO_2 on wet surfaces[10] or soot particles.[17,18] Recent studies suggest that $HONO_{(g)}$ was the major product of surface adsorbed and particulate NO_3^- photolysis,[19–21] which is surprising since the known aqueous phase photochemistry predicts nitrite formation to be a relatively minor photolysis channel. However, there is still a significant missing daytime source of $HONO_{(g)}$,[13,22] which limits the accuracy of models used to predict and study air pollution and changes to the global climate system.

Superoxide radical (and its conjugate base HO_2) has recently been hypothesized to play a role in $HONO_{(g)}$ emission enhancement from nitrate photolysis in environmental systems. Scharko et al. postulated the reaction between $HO_2/O_2^-{}_{(aq)}$, formed from organic compound oxidation, and $NO_{2(aq)}$ is a significant pathway, up to 20%, for aqueous NO_2 to NO_2^- conversion via the intermediate production and decomposition of aqueous peroxynitrate ($OONO_2^-$).[4] However, to our

knowledge no studies have attempted to prove this mechanism by direct measurement of $HO_2/O_2^-_{(aq)}$ concentrations in combination with nitrogen photoproducts during nitrate photolysis in solutions with dissolved organic matter.

We investigate herein the yields of NO_2(g), HONO(g) from nitrate photolysis, and provide the first direct measurements of O_2^-(aq) from nitrate photochemistry in the presence and absence of carboxylic acids and alcohols used to represent dissolved aliphatic organic matter (DAOM) found in environmental aqueous systems. These results articulate a critical secondary mechanism to explain enhanced $HONO_{(g)}$ emission from nitrate photolysis and suggest a key role of $O_2^-_{(aq)}$ and DAOM in atmospheric multiphase chemistry.

EXPERIMENTAL

Photochemical experiments were conducted with batch reactors containing phosphate buffered solutions (pH ~6) of nitrate in the presence and absence of aliphatic carboxylic acids or alcohols. Static solutions were irradiated using optically filtered Hg-Xe arc lamps ($\lambda > 295$ nm). Zero air was flowed through the headspace to detect $HONO_{(g)}$ and $NO_{x(g)}$ using a long path absorption photometer (QUMA, Model LOPAP-03) and chemiluminescence analyzer (CLD 88CYp), respectively. Reported NO_y concentrations have not been corrected for secondary photolysis, which amounted to 0.7–2% and 2–7% for HONO(g) and NO_2(g), respectively. Potential gaseous reaction interferences are listed in Table S3, although their influence is expected to be negligible. In separate experiments, superoxide was quantitated *in situ* with a flow injection chemiluminescence (FIC) analyzer (FeLume, Waterville Analytical; Figure S1B).[23] These samples were stirred to reproducibility measure aqueous superoxide. The chemiluminescence probe, methyl cypridina luciferin analog (MCLA), was used to selectively trap dissolved O_2^-/HO_2.[24–27] Additional

experimental details are provided in the Supplementary Information and described in detail elsewhere.[28]

RESULTS AND DISCUSSION

NO_2 and HONO Production. Experiments were conducted with 1 mM of surface-active DAOM surrogates that form an organic film at the air-water interface under static conditions. Irradiation of phosphate-buffered NO_3^- solutions with or without nonanoic acid (NNA, 1 mM, pH=5.8) or 1-octanol (1 mM, pH=6.0) produced statistically similar concentrations of gaseous NO_2 (Figures 1A and S3A). Integration of these data, after baseline subtraction of average pre-photolysis concentrations, reveals a 9% enhancement in $NO_{2(g)}$ emission rate in the presence of NNA, whereas 1-octanol caused an 8% decrease in $NO_{2(g)}$ emission rate (Table S1). This supports observations by Reeser et al[29] who showed that the $NO_{2(g)}$ yield from static nitrate photolysis experiments is sensitive to organic matter: 1-octanol lowered NO_2 emission relative to pure nitrate solutions, while octanoic acid increased $NO_{2(g)}$ emission. Reeser and coworkers suggest this is due to organic surface films affecting $NO_{2(g)}$ partitioning, although our results indicate that secondary photochemistry also plays a role. Specifically, while 1-octanol and nonanoic acid are both effective OH scavengers, 1-octanol leads to two times more $O_2^{\bullet-}{}_{(aq)}$ production than does nonanoic acid (Figure S4). Both $HO_{x(aq)}$ species react quickly with $NO_{2(aq)}$, although in the case of the 1-octanol system, higher $O_2^{\bullet-}{}_{(aq)}$ concentrations result in a lower steady-state $NO_{2(g)}$ concentration.

As shown in Figure 1B, photochemical $HONO_{(g)}$ production from nitrate solutions containing surface-active organics is enhanced relative to pure nitrate solutions. Nitrous acid formed in pure NO_3^- solutions reaches a steady-state, in contrast to the faster rate of HONO accumulation in the presence of the OH scavengers. For example, between 20–75 min, the $HONO_{(g)}$

emission rate for solutions containing NNA and 1-octanol is a factor of 2.4 and 3.2 higher, respectively, relative to the pure NO_3^- solution (Table S1). This is consistent with the view that $OH_{(aq)}$ reacts with $HONO_{(aq)}$ to limit its accumulation.[3–6]

To elucidate the role of DAOM solubility on product yields, we carried out similar experiments on homogeneous solutions containing one of several highly water-soluble organics: acetic (pH=5.7), propionic (pH=5.7), and valeric acids (pH=5.7), and ethanol (pH=6.0). Relative to the pure nitrate solution, emission of $NO_{2(g)}$ and $HONO_{(g)}$ were changed by a factor of between 0.58–1.01 for $NO_{2(g)}$ and 1.96–4.10 for $HONO_{(g)}$. Concentration ranges for $NO_{2(g)}$ and $HONO_{(g)}$ were comparable to experiments with surface-active organics, although different temporal trends for $NO_{2(g)}$ were observed (Figures 1C and D). At t= 20 min, the amount of $NO_{2(g)}$ generated in the presence of soluble organics was only half of what was generated in the presence of surface-active organic molecules; subsequently, $NO_{2(g)}$ concentration increased at a constant rate, reaching concentrations between 4–8 ppb by t=75 min. Differences in DAOM mixing, HO_x accumulation rates, and consumption of DAOM over time are likely responsible for observed differences in $NO_{2(g)}$ trends in Figure 1A, C, as discussed further in Section S7. The increasing trend in $HONO_{(g)}$ emission observed over the course of all experiments is due to the accumulation of $NO_2^-{}_{(aq)}$ and the slow diffusion of $HONO_{(g)}$ out of the solution under static conditions.

On average, secondary chemistry throughout the bulk solution leads to ~27% increase (p < 0.05) in the HONO:NO_2 ratio ($R_{enhance}$, Table S1) for homogenous DAOM solutions. Compared to DAOM solutions with surface active organics (1-octanol and NNA), solutions of water soluble DAOM species produced on average 19±4% (p<0.001) less $NO_{2(g)}$ and 6.0±2.1% (p<0.5) more $HONO_{(g)}$. Note that differences in HONO emissions between DAOM types were not statistically significant, which was due to the large standard deviation between the HONO(g) data from

different homogenous DAOM species. Ethanol and propionic acid solutions yield a faster HONO(g) emission and therefore better NO_2-to-HONO conversion rates than surface-active DAOM solutions, whereas acetic and valeric acid solutions emit $HONO_{(g)}$ more slowly (Figure 1D, Table S1). Regardless of DAOM type, our data agrees with a study by Scharko et al. which exhibited a suppression of $NO_{2(g)}$ yields from nitrate photolysis in the presence of water-soluble organic molecules due to secondary chemistry converting $NO_{2(aq)}$ to $HONO_{(aq)}$.[4,16] Notably, this is a static multiphase system; other possible factors impacting $NO_{2(g)}$ and $HONO_{(g)}$ levels are discussed in section S7.

O_2^- Production. Production of $HONO_{(g)}$ from nitrate photolysis in the presence of DAOM is hypothesized to involve $HO_2/O_2^-{}_{(aq)}$ as an intermediate.[4,5] We tested this hypothesis by measuring the concentration profiles for $O_2^-{}_{(aq)}$ formed when nitrate solutions were photolyzed with UV-visible radiation (Figure S4). Irradiation of each phosphate buffered solution (pH=6) yielded a burst in $O_2^-{}_{(aq)}$ concentration that quickly reached a maximum, followed by slight decline to quasi-steady-state levels. Photolysis of aqueous nitrate alone produces superoxide (~10 nM). This likely originates from production[5,7] and subsequent photolysis of peroxynitrous acid (HOONO) to form $NO_{(aq)}$ and $HO_{2(aq)}$ (Scheme 1a).[30–33] The addition of NNA (pH=6.0) or 1-octanol (pH=6.0) to nitrate solutions enhances $O_2^-{}_{(aq)}$ production 3- and 5-fold, respectively, relative to pure nitrate solutions, whereas blanks experiments do not produce significant amounts of superoxide (Figure S5). This $O_2^-{}_{(aq)}$ enhancement agrees well with the 2- to 5-fold enhancement ($R_{enhance}$) in HONO:NO_2 ratios observed for nitrate solutions containing organic solutes (see Table S1), indicating a potential link between HONO(g) formation and $HO_2/O_2^-{}_{(aq)}$ chemistry.

We therefore measured the response of $NO_{y(g)}$ species to increases in $HO_2/O_2^-{}_{(aq)}$ that occur when ethanol is added to photolyzed solutions of nitrate and NNA. As shown in Figure 2,

photolysis of nitrate and NNA forms O_2^-(aq), NO_2(g), HONO(g), and NO(g). Production of NO(g) is accounted for by the photolysis of NO_2^-/HONO [j(HONO)=5.0×10^{-3} s^{-1}] and NO_2 [j(NO_2)=1.6×10^{-2} s^{-1}] in the photochemical cell, as described in Section S8. Titration with ethanol simultaneously increases $HONO_{(g)}$ and $O_2^-{}_{(aq)}$ while decreasing $NO_{2(g)}$ and $NO_{(g)}$ concentrations. Furthermore, the total amount of excess $HONO_{(g)}$ accumulated (+45 ppb) is roughly equal to the total loss of $NO_{x(g)}$ (−56 ppb) observed. Plotting the total amount of $HONO_{(g)}$ produced vs. total $NO_{x(g)}$ consumed (Figure S6) shows that ~80% of the $NO_{x(g)}$ formed during the titrations is converted to HONO(g); the missing 20% is likely retained in solution as $NO_2^-{}_{(aq)}$. Sharp increases in superoxide occur immediately before significant jumps in the HONO:NO_x ratio (Figure S7), supporting the hypothesis that reaction of $HO_2/O_2^-{}_{(aq)}$ and $NO_{x(aq)}$ are responsible for the observed $HONO_{(g)}$ emission enhancement.

O_2^- and HONO Production Mechanism. It is well known that organic matter scavenges $OH_{(aq)}$ produced from the photolysis of NO_3^-.[4,5] Lower $OH_{(aq)}$ concentrations impede reactions (1)–(3) and consequently increase the amount of $NO_{2(aq)}$ and HONO/$NO_2^-{}_{(aq)}$ formed.

$$NO_2^- + OH \rightarrow NO_2 + OH \qquad k_5=1\times10^{10}\ M^{-1}\ s^{-1} \qquad (1)$$

$$HONO + OH \rightarrow NO_2 + H_2O \qquad k_6=3\times10^{9}\ M^{-1}\ s^{-1} \qquad (2)$$

$$NO_2 + OH \rightarrow H^+ + NO_3^- \qquad k_7=4.5\times10^{9}\ M^{-1}\ s^{-1} \qquad (3)$$

The lowest $NO_{2(g)}$ yield is indeed observed for acetic acid which has the slowest reaction with $OH_{(aq)}$ (Table S2), while $NO_{2(g)}$ yield is higher for ethanol or valeric acid, which are the most reactive DAOM species (Figure 1C). However, our results show that homogenous organics lead to a lower initial concentration of $NO_{2(g)}$ compared to pure nitrate solution photolysis (Figure 1A and C, t=20 min), indicating that secondary chemistry involving species such as $HO_2/O_2^-{}_{(aq)}$ significantly affect the dissolved concentration of $NO_{2(aq)}$.

The data support that reactions of $NO_{x(aq)}$ with $O_2^-{}_{(aq)}$ are significant pathways by which $HONO_{(aq)}$ production is enhanced by DAOM. Superoxide reacts rapidly with $NO_{2(aq)}$ (k=4.5×10^9 M^{-1} s^{-1}),[1,7,34] to form peroxynitrate ($OONO_2^-$), which thermally decomposes to form $NO_2^-{}_{(aq)}$ and $O_{2(aq)}$ (1.4 s^{-1}, Scheme 1c).[35,36] Rapid reaction between $O_2^-{}_{(aq)}$ and $NO_{(aq)}$ (4.3×10^9 M^{-1} s^{-1}, Scheme 1d)[37] is expected to be an additional pathway to $NO_2^-{}_{(aq)}$ formation. The product, peroxynitrite ($OONO^-$), may either undergo internal rearrangement to form NO_3^- (1.0 s^{-1}),[7] or disproportionate to form $NO_2^-{}_{(aq)}$ and $HOONO_{2(aq)}$ (3.0×10^4 M^{-1} s^{-1}).[38] Therefore, the enhanced levels of $O_2^-{}_{(aq)}$ would react with $NO_{x(aq)}$ and lead to higher $HONO_{(g)}$ emissions from DAOM solutions relative to what is seen for pure nitrate solutions. Notably, the combined production rate of $HONO_{(g)}$ and $NO_{2(g)}$ [P(NO_2 + HONO), Table S1] is similar for all nitrate solutions, regardless of whether organics are present. This indicates that the HONO(g) enhancement in solutions containing organic compounds is due to a shift in the product distribution from $NO_{2(g)}$ to $HONO_{(g)}$ rather than a change in the rate of product formation from NO_3^- photolysis.

Influence of RO_2 on measured species. Differences in NO_x-to-HONO conversion between different DAOM surrogates in Figure 1 are likely due to secondary reactions impacting $O_2^-{}_{(aq)}$ levels. Reactions between $OH_{(aq)}$ with DAOM leads to alkylperoxy radicals (RO_2), which form $O_2^-/HO_{2(aq)}$ via mechanisms that depend on $RO_{2(aq)}$ structure. Alcohols react with $OH_{(aq)}$ to preferentially form α-hydroperoxyl radicals (Scheme 1b), which decompose unimolecularly to $HO_{2(aq)}$, with rate constants that increase with degree of methyl substitution.[39] This unimolecular decomposition could explain the higher $HONO_{(aq)}$ concentrations in the presence of ethanol (Figure 1D). Carboxylic acid peroxyl radicals form less $HO_{2(aq)}$ due to their stability and propensity to dimerize; the dimers eventually decompose to release $HO_2/O_2^-{}_{(aq)}$ (Scheme 1b).[40,41] However, the system is more complicated since peroxyl radicals may further act as $O_2^-{}_{(aq)}$ and $NO_{x(aq)}$ sinks that

yield alkyl hydroperoxyl radicals and organic nitrates/nitrites.[40,42,43] This may explain the trends observed for acetic, propionic, and valeric acids. Carboxylic acids with shorter alkyl chains have slower $OH_{(aq)}$ reaction rates (Table S2), which seems to correspond to lower $NO_{2(g)}$ emissions since more $OH_{(aq)}$ is available to oxidize $NO_{2(aq)}$. Differences in $HONO_{(g)}$ production do not follow the same trend, likely due to unknown differences in $RO_{2(aq)}$ stability and reactivity towards $NO_{2(aq)}$, $NO_{(aq)}$, and $O_2^-{}_{(aq)}$. All considerations point toward the central role of $RO_{2(aq)}$ decomposition and reactivity toward $HO_2/O_2^-{}_{(aq)}$, or $NO_{x(aq)}$, which are insufficiently defined and warrant future investigations.

Environmental Implications. The presented work illustrates that nitrate photolysis in the actinic range ($\lambda > 290$ nm) produces $HO_2/O_2^-{}_{(aq)}$ and $HONO_{(g)}$ in the presence of DAOM, with an enhancement steming from secondary photochemistry between $O_2^-/HO_{2(aq)}$ and photoproduced $NO_{x(aq)}$. Using production rate of NO_2 and HONO as proxies for the nitrate photolysis rate, the observed $j(NO_3^-)$ are not significantly different from one another (Table S4), regardless whether organics are present, indicating the role of DAOM is to increase the $HONO/NO_2^-{}_{(aq)}$ yield at the expense of $NO_{x(aq)}$. Previous studies focused on the importance of HONO production from aerosol nitrate and nitric acid use enhancement factors (EF) [i.e., the ratio of $j(NO_3^-)$ in the aerosol phase to $j(HNO_3)$ in the gas phase] to describe release of HONO and NO_x from aerosol nitrate photolysis. As shown in Table S4, the EF calculated for pure nitrate and nitrate in the presence of organic molecules indicates an overall slower rate of $NO_3^-{}_{(aq)}$ photolysis relative to $HNO_{3(g)}$. This reflects the factor of 10 lower quantum yield of nitrate photolysis in bulk solution compared to that of $HNO_{3(g)}$, which is due to rapid recombination of NO_3^-(aq) products in the solvent cage. Nitrate adsorbed to surfaces will have an incomplete solvent cage, leading to enhanced quantum yields.[44,45] Enhancement factors of 10–50 have been reported for HONO measurements in field

campaigns[21,46,47] which are likely due to surface nitrate photolysis occurring in the presence of organics. Importantly, reactions between NO_x and HO_2/O_2^- in the aerosol phase explain how colocation of nitrate with organic matter can translate the rate enhancement factor into the additional HONO production observed in the field. This chemistry is applicable to many aqueous environments (e.g., cloud droplets, aqueous aerosols, surface water) and may represent a significant source of HONO(g) in areas where surface waters or aqueous microlayers contain high concentration of nitrate and DAOM. This chemistry should therefore be considered in models for nitrate photochemistry and air quality.

SUPPORTING INFORMATION. Additional experimental details, discussion, 4 tables and 8 figures are provided. These include: materials; NO_x and HONO measurements; quantitation of O_2^-; factors impacting NO_2 and HONO; additional experiment involving titration of ethanol to irradiated NO_3^- solution; tabulated analysis of NO_2-to-HONO conversion for experiments; schematics of the experimental setup including lamp spectrum.

Notes

The authors declare no competing financial interest.

ACKNOWLEDEMENTS

Work at IRCELYON project was supported by the ANR-RGC programme (project ANR-16-CE01-0013, A-PolyU502/16). Work at Indiana University was supported by grants from the U.S. National Science Foundation (NSF) (AGS-1352375 and CHE-1609752). E.Z.D. was supported by a U.S. NSF Graduate Research Fellowship (2019286041). We are grateful to Prof. Whitney King (Colby College) for helpful discussions regarding the FIC analyzer.

REFERENCES

(1) Mack, J.; Bolton, J. R. Photochemistry of Nitrite and Nitrate in Aqueous Solution: A Review. *J. Photochem. Photobiol. A Chem.* **1999**, *128* (1–3), 1–13.

(2) Herrmann, H. On the Photolysis of Simple Anions and Neutral Molecules as Sources of O-/OH, SOx- and Cl in Aqueous Solution. *Phys. Chem. Chem. Phys.* **2007**, *9* (30), 3935–3964.

(3) Roca, M.; Zahardis, J.; Bone, J.; El-Maazawi, M.; Grassian, V. H. 310 Nm Irradiation of Atmospherically Relevant Concentrated Aqueous Nitrate Solutions: Nitrite Production and Quantum Yields. *J. Phys. Chem. A* **2008**, *112* (51), 13275–13281.

(4) Scharko, N. K.; Berke, A. E.; Raff, J. D. Release of Nitrous Acid and Nitrogen Dioxide from Nitrate Photolysis in Acidic Aqueous Solutions. *Environ. Sci. Technol.* **2014**, *48* (20), 11991–12001.

(5) Benedict, K. B.; McFall, A. S.; Anastasio, C. Quantum Yield of Nitrite from the Photolysis of Aqueous Nitrate above 300 Nm. *Environ. Sci. Technol.* **2017**, *51* (8), 4387–4395.

(6) Zellner, R.; Exner, M.; Herrmann, H. Absolute OH Quantum Yields in the Laser Photolysis of Nitrate, Nitrite and Dissolved H2O2 at 308 and 351 Nm in the Temperature Range 278?353 K. *J. Atmos. Chem.* **1990**, *10* (4), 411–425.

(7) Løgager, T.; Sehested, K. Formation and Decay of Peroxynitric Acid: A Pulse Radiolysis Study. *J. Phys. Chem.* **1993**, *97* (39), 10047–10052.

(8) Xue, L.; Gu, R.; Wang, T.; Wang, X.; Saunders, S.; Blake, D.; Louie, P. K. K.; Luk, C. W. Y.; Simpson, I.; Xu, Z.; et al. Oxidative Capacity and Radical Chemistry in the Polluted Atmosphere of Hong Kong and Pearl River Delta Region: Analysis of a Severe Photochemical Smog Episode. *Atmos. Chem. Phys.* **2016**, *16* (15), 9891–9903.

(9) Harris, G. W.; Carter, W. P. L.; Winer, A. M.; Pitts, J. N.; Platt, U.; Perner, D. Observations of Nitrous Acid in the Los Angeles Atmosphere and Implications for Predictions of Ozone-Precursor Relationships. *Environ. Sci. Technol.* **1982**, *16* (7), 414–419.

(10) Finlayson-Pitts, B. J.; Wingen, L. M.; Sumner, A. L.; Syomin, D.; Ramazan, K. A. The Heterogeneous Hydrolysis of NO2 in Laboratory Systems and in Outdoor and Indoor Atmospheres: An Integrated Mechanism. *Phys. Chem. Chem. Phys.* **2003**, *5* (2), 223–242.

(11) Oswald, R.; Behrendt, T.; Ermel, M.; Wu, D.; Su, H.; Cheng, Y.; Breuninger, C.; Moravek, A.; Mougin, E.; Delon, C.; et al. HONO Emissions from Soil Bacteria as a Major Source of Atmospheric Reactive Nitrogen. *Science (80-.).* **2013**, *341* (6151), 1233–1235.

(12) Tong, S.; Hou, S.; Zhang, Y.; Chu, B.; Liu, Y.; He, H.; Zhao, P.; Ge, M. Exploring the Nitrous Acid (HONO) Formation Mechanism in Winter Beijing: Direct Emissions and Heterogeneous Production in Urban and Suburban Areas. *Faraday Discuss.* **2016**, *189*, 213–230.

(13) Lee, J. D.; Whalley, L. K.; Heard, D. E.; Stone, D.; Dunmore, R. E.; Hamilton, J. F.; Young, D. E.; Allan, J. D.; Laufs, S.; Kleffmann, J. Detailed Budget Analysis of HONO in Central London Reveals a Missing Daytime Source. *Atmos. Chem. Phys.* **2016**, *16* (5), 2747–2764.

(14) Kleffmann, J. Daytime Sources of Nitrous Acid (HONO) in the Atmospheric Boundary Layer. *ChemPhysChem* **2007**, *8* (8), 1137–1144.

(15) George, C.; Strekowski, R. S.; Kleffmann, J.; Stemmler, K.; Ammann, M. Photoenhanced Uptake of Gaseous NO2 on Solid Organic Compounds: A Photochemical Source of

HONO? *Faraday Discuss.* **2005**, *130* (2), 195.
(16) Stemmler, K.; Ammann, M.; Donders, C.; Kleffmann, J.; George, C. Photosensitized Reduction of Nitrogen Dioxide on Humic Acid as a Source of Nitrous Acid. *Nature* **2006**, *440* (7081), 195–198.
(17) Han, C.; Liu, Y.; He, H. Heterogeneous Reaction of NO2 with Soot at Different Relative Humidity. *Environ. Sci. Pollut. Res.* **2017**, *24* (26), 21248–21255.
(18) Monge, M. E.; D'Anna, B.; Mazri, L.; Giroir-Fendler, A.; Ammann, M.; Donaldson, D. J.; George, C. Light Changes the Atmospheric Reactivity of Soot. *Proc. Natl. Acad. Sci. U. S. A.* **2010**, *107* (15), 6605–6609.
(19) Zhou, X.; Zhu, L. Role of Nitric Acid Surface Photolysis on Tropospheric Cycling of Reactive Nitrogen Species. *Adv. Atmos. Chem.* **2016**, *1* (2), 271–304.
(20) Zhou, X.; Gao, H.; He, Y.; Huang, G.; Bertman, S. B.; Civerolo, K.; Schwab, J. Nitric Acid Photolysis on Surfaces in Low-NOx Environments: Significant Atmospheric Implications. *Geophys. Res. Lett.* **2003**, *30* (23), 10–13.
(21) Romer, P. S.; Wooldridge, P. J.; Crounse, J. D.; Kim, M. J.; Wennberg, P. O.; Dibb, J. E.; Scheuer, E.; Blake, D. R.; Meinardi, S.; Brosius, A. L.; et al. Constraints on Aerosol Nitrate Photolysis as a Potential Source of HONO and NOx. *Environ. Sci. Technol.* **2018**, *52* (23), 13738–13746.
(22) Kleffmann, J.; Gavriloaiei, T.; Hofzumahaus, A.; Holland, F.; Koppmann, R.; Rupp, L.; Schlosser, E.; Siese, M.; Wahner, A. Daytime Formation of Nitrous Acid: A Major Source of OH Radicals in a Forest. *Geophys. Res. Lett.* **2005**, *32* (5), 1–4.
(23) King, D. W.; Lounsbury, H. a; Millero, F. Rates Aml Mechanism of Fe(Ll) Iron Concentrations. *Environ. Sci. Technol.* **1995**, *29* (3), 818–824.
(24) Akutsu, K.; Nakajima, H.; Katoh, T.; Kino, S.; Fujimori, K. Chemiluminescence of Cipridina Luciferin Analogues. Part 2. Kinetic Studies on the Reaction of 2-Methyl-6-Phenylimidazo[1,2-a]Pyrazin-3(7H)-One (CLA) with Superoxide: Hydroperoxyl Radical Is an Actual Active Species Used to Initiate the Reaction. *J. Chem. Soc. Perkin Trans. 2* **1995**, No. 8, 1699.
(25) Fujimori, K.; Nakajima, H.; Akutsu, K.; Mitani, M.; Sawada, H.; Nakayama, M. Chemiluminescence of Cypridina Luciferin Analogues. Part 1. Effect of PH on Rates of Spontaneous Autoxidation of CLA in Aqueous Buffer Solutions. *J. Chem. Soc. Perkin Trans. 2* **1993**, No. 12, 2405.
(26) Rose, A. L.; Moffett, J. W.; Waite, T. D. Determination of Superoxide in Seawater Using 2-Methyl-6-(4-Methoxyphenyl)- 3,7-Dihydroimidazo[1,2-a]Pyrazin-3(7H)-One Chemiluminescence. *Anal. Chem.* **2008**, *80* (4), 1215–1227.
(27) Rose, A. L.; Webb, E. A.; Waite, T. D.; Moffett, J. W. Measurement and Implications of Nonphotochemically Generated Superoxide in the Equatorial Pacific Ocean. *Environ. Sci. Technol.* **2008**, *42* (7), 2387–2393.
(28) Wang, X.; Gemayel, R.; Hayeck, N.; Perrier, S.; Charbonnel, N.; Xu, C.; Chen, H.; Zhu, C.; Zhang, L.; Wang, L.; et al. Atmospheric Photosensitization: A New Pathway for Sulfate Formation. *Environ. Sci. Technol.* **2020**, acs.est.9b06347.
(29) Reeser, D. I.; Kwamena, N. O. A.; Donaldson, D. J. Effect of Organic Coatings on Gas-Phase Nitrogen Dioxide Production from Aqueous Nitrate Photolysis. *J. Phys. Chem. C* **2013**, *117* (43), 22260–22267.
(30) Vione, D.; Maurino, V.; Minero, C.; Pelizzetti, E. Reactions Induced in Natural Waters by Irradiation of Nitrate and Nitrite Ions. *Environ. Photochem. Part II* **2005**, *2* (September), 221–253.

(31) Sturzbecher-Höhne, M.; Nauser, T.; Kissner, R.; Koppenol, W. H. Photon-Initiated Homolysis of Peroxynitrous Acid. *Inorg. Chem.* **2009**, *48* (15), 7307–7312.
(32) Goldstein, S.; Lind, J.; Merényi, G. Chemistry of Peroxynitrites as Compared to Peroxynitrates. *Chem. Rev.* **2005**, *105* (6), 2457–2470.
(33) Abida, O.; Mielke, L. H.; Osthoff, H. D. Observation of Gas-Phase Peroxynitrous and Peroxynitric Acid during the Photolysis of Nitrate in Acidified Frozen Solutions. *Chem. Phys. Lett.* **2011**, *511* (4–6), 187–192.
(34) Bielski, B. H. J.; Cabelli, D. E.; Arudi, R. L.; Ross, A. B. Reactivity of HO2/O2− Radicals in Aqueous Solution. *J. Phys. Chem. Ref. Data* **1985**, *14* (4), 1041–1100.
(35) Lammel, G.; Ferner, D.; Warneck, P. Decomposition of Pernitric Acid in Aqueous Solution. *J. Phys. Chem.* **1990**, *94* (15), 6141–6144.
(36) Goldstein, S.; Czapski, G.; Lind, J.; Merenyi, G. Mechanism of Decomposition of Peroxynitric Ion (O2NOO-): Evidence for the Formation. *Inorg. Chem.* **1998**, *37* (16), 3943–3947.
(37) Goldstein, S.; Czapski, G. The Reaction of NO· with O2·- and HO2·-: A Pulse Radiolysis Study. *Free Radic. Biol. Med.* **1995**, *19* (4), 505–510.
(38) Gupta, D.; Harish, B.; Kissner, R.; Koppenol, W. H. Peroxynitrate Is Formed Rapidly during Decomposition of Peroxynitrite at Neutral PH. *Dalt. Trans.* **2009**, No. 29, 5730–5736.
(39) von Sonntag, C.; Schuchmann, H. -P. The Elucidation of Peroxyl Radical Reactions in Aqueous Solution with the Help of Radiation-chemical Methods. *Angew. Chemie Int. Ed. English* **1991**, *30* (10), 1229–1253.
(40) Schuchmann, M. N.; Zegota, H.; Sonntag, C. von. Acetate Peroxyl Radicals, ·O2CH2 CO2-: A Study on the γ-Radiolysis and Pulse Radiolysis of Acetate in Oxygenated Aqueous Solutions. *Zeitschrift für Naturforsch. B* **1985**, *40* (2), 215–221.
(41) Karpel Vel Leitner, N.; Dore, M. Hydroxyl Radical Induced Decomposition of Aliphatic Acids in Oxygenated and Deoxygenated Aqueous Solutions. *J. Photochem. Photobiol. A Chem.* **1996**, *99* (2–3), 137–143.
(42) Schuchmann, M. N.; Schuchmann, H. P.; Von Sonntag, C. The PKa Value of the (Carboxymethyl)Peroxyl Radical: The Taft Σ* Constant of the -CH2O2· Group. *J. Phys. Chem.* **1989**, *93* (13), 5320–5323.
(43) Goldstein, S.; Lind, J.; Merenyi, G. Reaction of Organic Peroxyl Radicals with ·NO2 and ·NO in Aqueous Solution: Intermediacy of Organic Peroxynitrate and Peroxynitrite Species. *J. Phys. Chem. A* **2004**, *108* (10), 1719–1725.
(44) Nissenson, P.; Knox, C. J. H.; Finlayson-Pitts, B. J.; Phillips, L. F.; Dabdub, D. Enhanced Photolysis in Aerosols: Evidence for Important Surface Effects. *Phys. Chem. Chem. Phys.* **2006**, *8* (40), 4700–4710.
(45) Wingen, L. M.; Moskun, A. C.; Johnson, S. N.; Thomas, J. L.; Roeselová, M.; Tobias, D. J.; Kleinman, M. T.; Finlayson-Pitts, B. J. Enhanced Surface Photochemistry in Chloride-Nitrate Ion Mixtures. *Phys. Chem. Chem. Phys.* **2008**, *10* (37), 5668–5677.
(46) Kasibhatla, P.; Sherwen, T.; Evans, M. J.; Carpenter, L. J.; Reed, C.; Alexander, B.; Chen, Q.; Sulprizio, M. P.; Lee, J. D.; Read, K. A.; et al. Global Impact of Nitrate Photolysis in Sea-Salt Aerosol on NOx, OH, and O3 in the Marine Boundary Layer. *Atmos. Chem. Phys.* **2018**, *18* (15), 11185–11203.
(47) Reed, C.; Evans, M. J.; Crilley, L. R.; Bloss, W. J.; Sherwen, T.; Read, K. A.; Lee, J. D.; Carpenter, L. J. Evidence for Renoxification in the Tropical Marine Boundary Layer. *Atmos. Chem. Phys.* **2017**, *17* (6), 4081–4092.

Figures

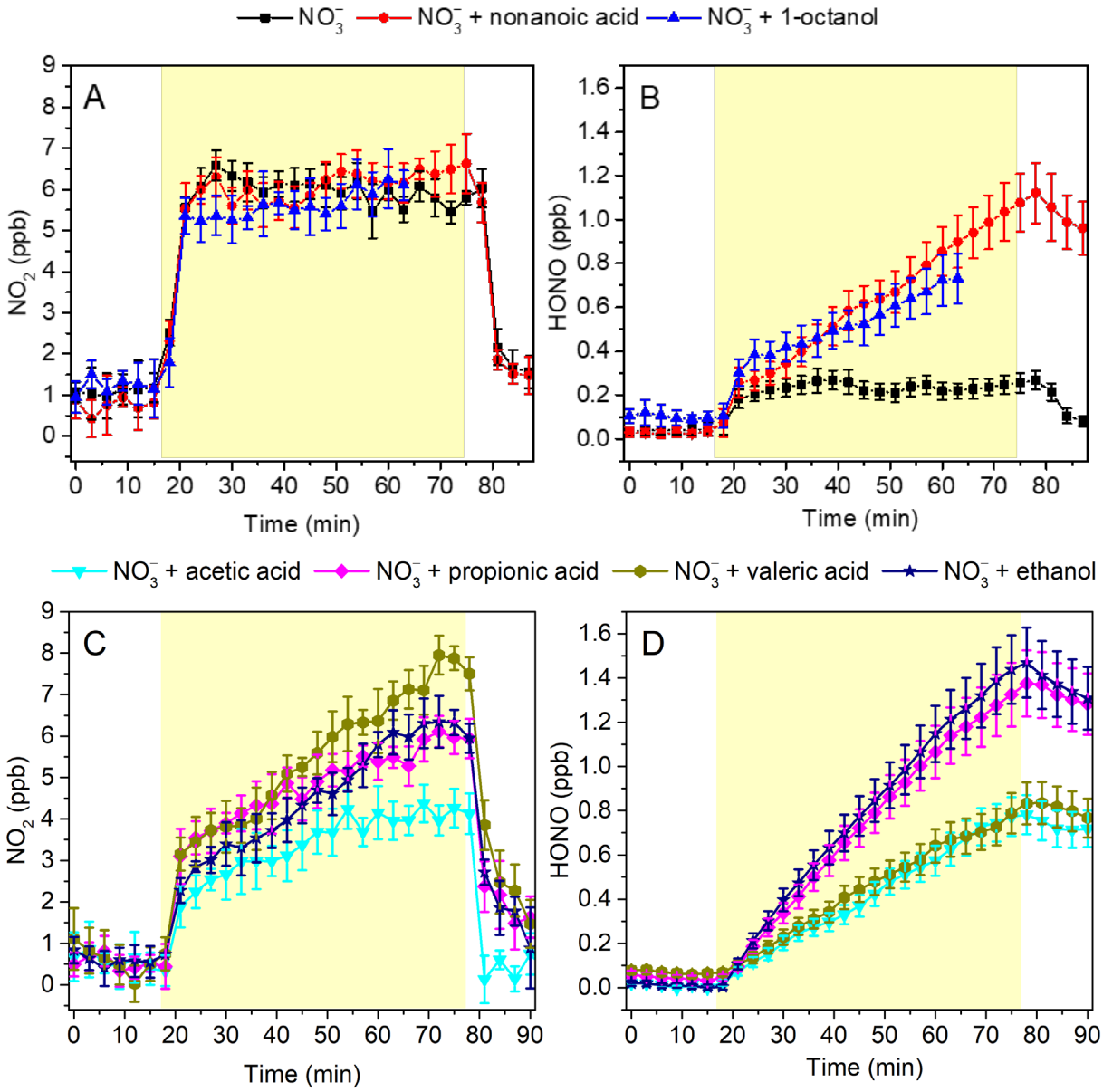

Figure. 1. NO_2(g) and HONO(g) concentration profiles during the irradiation of phosphate buffered nitrate solutions (pH 5.8 ± 0.2). The production of (A) NO_2(g) and (B) HONO(g) is in the presence or absence of NNA or 1-octanol, and the production of (C) NO_2(g) and (D) HONO(g) is in the presence of acetic acid, propionic acid, valeric acid, or ethanol, respectively. The yellow region corresponds to the irradiation period (duration 1 hour) starting at time = 16 min.

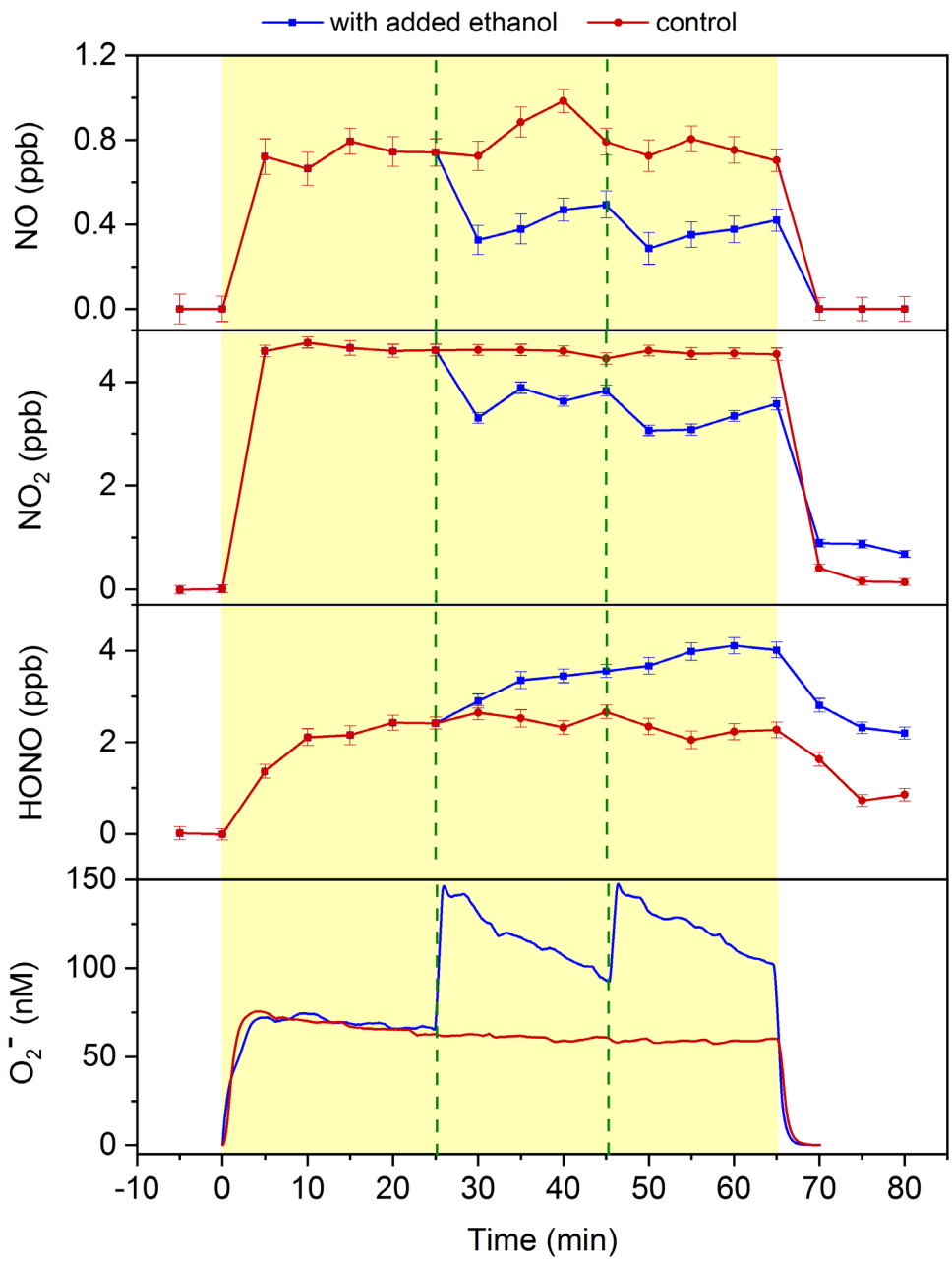

Figure 2. Simultaneous measurement of NO(g), NO_2(g), HONO(g), and O_2^-(aq) arising when solutions of nitrate and nonanoic acid (10 mM, 1 mM, pH 5) are irradiated with UV-visible light. Green dashed lines indicate points in time when 100 µL aliquots of a solution containing ethanol (1.5 M) and DTPA (50 µM) were added to initiate HO_2/O_2^-(aq) formation. For the control experiment, aliquots of DTPA (50 µM) alone was added to the control. The yellow region corresponds to the irradiation period.

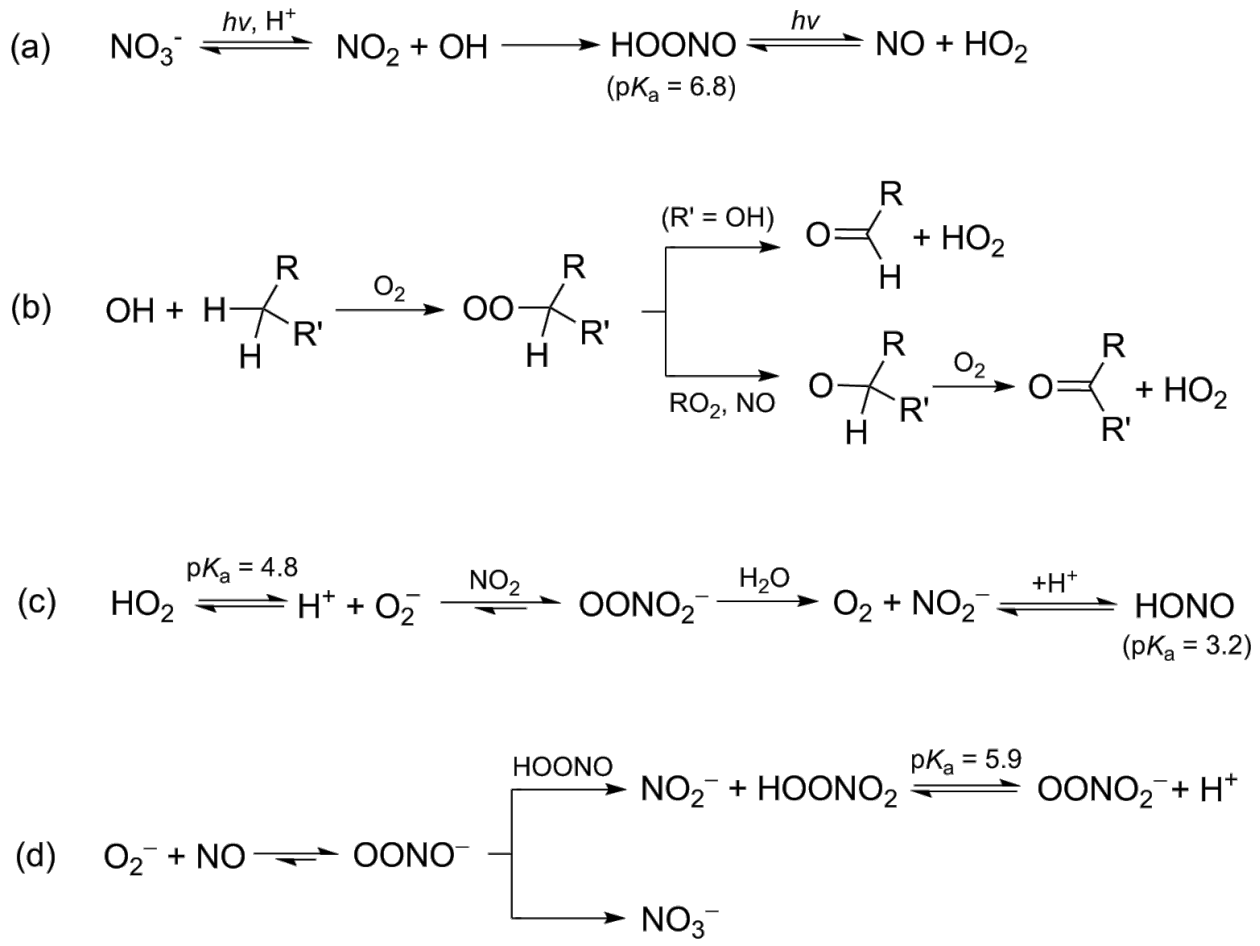

396

397 **Scheme 1.** Reaction mechanisms for $HO_2/O_2^-{}_{(aq)}$ and $NO_2^-{}_{(aq)}$ formation.

398

399

400

401

402

403

404

405

406

407

TOC

For Table of Contents Use Only

Title: Superoxide and nitrous acid production from nitrate photolysis is enhanced by dissolved aliphatic organic matter

Authors: Xinke Wang, Evan Z. Dalton, Zachary C. Payne, Sebastien Perrier, Matthieu Riva, Jonathan D. Raff, and Christian George